



Seismic Performance Evaluation of RC Bridges by IDA of Single-Run ESDOF and ISA

Prakit Chomchuen¹, Virote Boonyapinyo^{2,*}

¹*Department of Civil Engineering, School of Engineering and Industrial Technology,
Mahanakorn University of Technology, Bangkok 10530, Thailand*

²*Department of Civil Engineering, Faculty of Engineering, Thammasat School of Engineering,
Thammasat University, Pathum Thani 12120, Thailand*

Received 15 February 2023; Received in revised form 11 January 2024

Accepted 1 February 2024; Available online 31 March 2024

ABSTRACT

This study aims to present the applicability of incremental dynamic analysis (IDA) of equivalent single degree of freedom (ESDOF) and incremental static analysis (ISA) by incremental capacity spectrum method (ICSM) for evaluating the seismic performance of single column bridges. A lateral load pattern that includes higher mode effect for single-run displacement-based nonlinear static analysis to evaluate the lateral behavior of multi-degree of freedom (MDOF) analytical model is proposed. The failure criteria include the interaction of axial force and bidirectional moments, shear failure and column drift limit. The efficiency of the proposed load pattern is investigated through evaluating seismic performance of the typical single column bridge with three different column heights in Bangkok, Thailand. The results show that the different load patterns result in difference capacity and stiffness of ESDOF. The results also show that the IDA of ESDOF with the proposed load pattern can be used efficiently and accurately for all studied bridges compared with IDA of MDOF. Moreover, using IDA of ESDOF for evaluating the seismic performance of the studied bridges can reduce the computational time about 15 times per load case compared with IDA of MDOF. The ISA by ICSM also reduces the computational time because the nonlinear time history analysis is not required for this method. However, the ISA by ICSM shows acceptable results only for the studied bridge with high first-mode participating mass ratio. The results also show that the spectrum acceleration of MDOF at collapse are 0.746g, 1.130g, and 0.461g for the studied bridges with 4.5 m., 6.3 m., and 15 m. column heights, respectively.

Keywords: Incremental dynamic analysis; Incremental static analysis; Multi-mode combination load pattern; Seismic performance evaluation; Reinforced concrete bridge

1. Introduction

Nonlinear time history analysis (NTHA) is the most reliable seismic response evaluation method. Seismic responses are calculated by solving the equation of motion of the analytical model of the structure under the influence of a considered ground motion. Although NTHA is the most reliable method for seismic performance evaluation, it is also costly and time-consuming, especially when considering the complex behavior of structures, such as inelastic behavior. Therefore, it is impractical to use NTHA for evaluating the seismic performance of the structures. To make seismic performance evaluation more practical, more efficient methods based on nonlinear static analysis (NSA) have been proposed. One popular NSA-based method is the capacity spectrum method (CSM), which is documented in ATC-40 [1]. The CSM is a simple method that combines the lateral capacity of the structure with the seismic demand from the considered ground motion to evaluate the seismic performance. Three methods for evaluating the seismic performance by CSM are suggested in ATC-40 [1]: Methods A, B, and C.

Krawinkle and Seneviratna [2] found that the CSM gives accurate results compared with NTHA only when the behavior of the structure is dominated by the first fundamental mode of vibration. Chopra and Goel [3] also showed that the CSM has a convergence problem for some cases. To improve the capacity of NSA-based methods for evaluating seismic performance, several techniques have been proposed, such as the Inelastic Demand Diagram Method (IDDM) [4] and N2 [5].

Incremental Dynamic Analysis (IDA) was compiled and proposed by Vamvatsikos and Cornell [6]. It is a recently popular method for evaluating the seismic performance of structures because it provides the necessary information to assess the performance levels or limit states of the structures, which are important ingredients of Performance-Based Earthquake Engineering (PBEE). Therefore, IDA has attracted researchers and engineers to

use it as a tool for evaluating the seismic behavior of structures, e.g., Mander et al. [7], Vejdani-Noghreiyani and Shooshtari [8], Tehrani and Mitchell [9, 10], Alembagheri and Ghaemian [11], and Nazari and Bargi [12].

To evaluate the seismic performance of structures by IDA, two main tasks must be achieved: (1) evaluating the seismic demand under a set of ground motions by IDA, and (2) applying the capacity (limit state) to the demand to evaluate the probabilistic damage of the structures.

To avoid the time-consuming NTHA method for generating the IDA curve, another technique has been studied. Dolsek and Fajfar [13] proposed to adapt the N2 method for approximating the IDA curve, called incremental N2 (IN2). The seismic response or demand measure of the structure under each scaled ground motion was evaluated using the concept of the N2 method.

Although using NTHA to perform IDA of a multi-degree-of-freedom (MDOF) analytical model is the most reliable method, it is also the most computationally expensive. To reduce the computational cost and time of performing IDA of MDOF systems, the concept of the equivalent single-degree-of-freedom (ESDOF) system is adapted [14]. NSA of the MDOF system is performed to generate the lateral behavior of the structure. The generated lateral behavior of the MDOF system is defined as the force-displacement relationship of the ESDOF system. IDA of the ESDOF system is then performed to evaluate the seismic behavior of the structure.

However, using the result of conventional NSA as the lateral behavior of the ESDOF system means that the drawbacks of conventional NSA are still present in the IDA results, i.e., the effect of higher modes of vibration is not included in conventional NSA. Therefore, this method is not suitable for very flexible structures.

To account for the higher mode effects in IDA of ESDOF systems, modal incremental dynamic analysis (MIDA) has been investigated [15-23]. For the concept of

MIDA, modal pushover analysis is used to generate the modal lateral behavior of the structure, which is then applied to the ESDOF system to obtain the modal ESDOF. Then, multiple-run IDA for all modal ESDOFs is performed to evaluate the maximum modal displacement of each modal ESDOF. Finally, the maximum displacements of all modal ESDOFs are approximately combined using a modal combination rule.

Bridges are important structures and their seismic performance should be evaluated accurately. Therefore, the seismic performance of bridges by IDA viewpoint are increasingly interesting (e.g. Mander et al. [7], Felice and Giannini [24], Akbari [25], Sadan et al. [26], and Jeon et al. [27]). Although there are several researchers which study seismic performance evaluation of the bridges by IDA approach of MDOF, applying the concept of IDA of ESDOF for the bridges has been done only a few times and not yet been clearly expressed.

Therefore, this study aims to intensively investigate the applicability of IDA of ESDOF and incremental static analysis (ISA) by ICSM for evaluating the seismic performance of the single column bridges. In this research, a lateral load pattern that takes into account higher mode effect for single-run displacement-based NSA to evaluate the lateral behavior of MDOF is proposed. The efficiency of both methods is examined by evaluating the seismic performance of single-column reinforced concrete (RC) bridges with varying column heights.

2. Case Study of Single-Column Reinforced Concrete Bridges

Bridges are critical infrastructure that must be able to withstand earthquakes. Therefore, it is essential to accurately evaluate their seismic performance. Consequently, the seismic performance of bridges by IDA viewpoint are increasingly interesting (e.g. Mander et al. [7], Felice and Giannini [24], Akbari [25], Sadan et al. [26], and Jeon et al. [27]). Although, there are several researchers

who study seismic performance evaluation of the bridges by IDA approach of MDOF, applying the concept of IDA of ESDOF for the bridges is rarely done and not yet clearly expressed. The studied bridges are single-column reinforced concrete bridges on Expressway Phase 1 in Bangkok, Thailand, which were built in 1976.

Furthermore, single-column bridges are a common sight in Thailand, as seen in Fig. 1. These bridges exhibit a variety of column heights depending on their intended purpose. To investigate the effect of column flexibility on seismic of the bridges, this paper focus on three distinct column heights as parameters, as illustrated in Fig. 2.



Fig. 1. Various applications of single column RC bridges in Bangkok, Thailand.

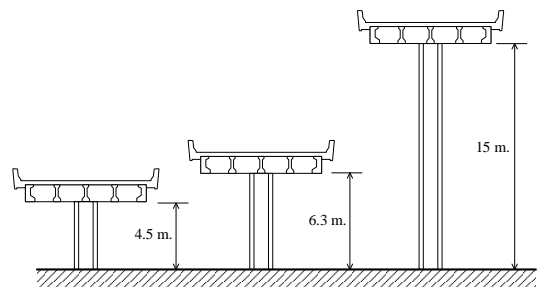


Fig. 2. Studied bridge with three different column heights.

2.1 General configurations and analytical model

A bridge's as-built drawing is a detailed specification of the structure. The design strength of concrete is 23.5 MPa. for in-situ

reinforced concrete and 34.32 MPa. for precast prestressed concrete beams. Grade 40 deformed bars are used for reinforcement. The studied bridges are divided into four components: superstructure, bearing system, substructure, and footing. The details of each component are described below, except for the footing, which is assumed to be a fixed support for all case studies.

2.1.1 Superstructure

The superstructure of the studied bridges comprises an 18-centimeter-thick reinforced concrete slab placed on the top of five pre-stressed concrete I-girders as shown in Fig. 3. This superstructure is treated as elastic and is modeled as lumped single elastic beam-column elements. According to the bridges modeling for nonlinear analysis proposed by Aviram [28], in this study, the lumped beam-column elements were subdivided into four elements per span. The translational mass of the superstructure is automatically computed and lumped into the nodes of the beam-column elements. Additionally, torsional masses, which significantly impact the dynamic characteristics of the bridges, especially in the transverse direction, were computed and allocated to the element nodes.

2.1.2 Bearing system

The studied bridges used an elastomeric bearing pad system as bearing systems as shown in Fig. 4(a). This system is represented within the analytical model as an elastic spring element with six degrees of freedom as illustrated in Fig. 4(b). The stiffness values for each of these degrees of freedom are computed in accordance with the beam theory methodology advocated by Yazdani et al. [29]. The literature reveals that the shear modulus of

rubber is contingent upon its hardness. To accurately model realistic behavior, it is essential to assess the hardness of the rubber. A report from the Thammasat University Research and Consultancy Institute [30] concerning an inspection of the bearing pads on an expressway in Bangkok indicates that the rubber hardness of these bearing pads measures approximately 60 Shore A on the hardness scale. According to AASHTO guidelines [31], an appropriate shear modulus for new rubber with a hardness of 60 Shore A is estimated to be 0.9 MPa. Although the stiffness of bearing pad can be calculated directly from specified material properties of new rubber suggested in AASHTO [31], Yazdani et al. [29] have shown that elastomers can experience significant stiffening due to aging and exposure to cold temperatures. This stiffening effect can result in stiffness values up to 50 times greater than the original stiffness. The stiffness values for the bearing pads in this study are summarized in Table 1.

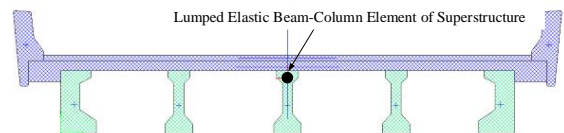


Fig. 3. Superstructure of the studied bridges.

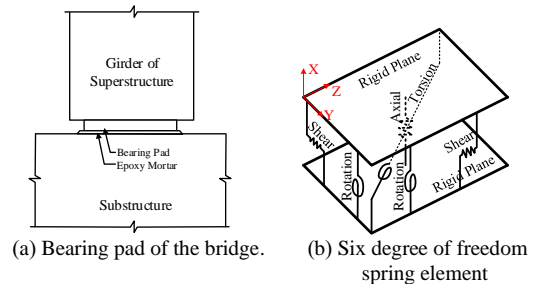


Fig. 4. Bearing system modeling.

Table 1. Stiffness of bearing pad in six directions.

Axial Stiffness (KX) (kN/mm)	Shear Stiffness in Y direction (KY) (kN/mm)	Shear Stiffness in Z direction (KZ) (kN/mm)	Torsional Stiffness about X (KRX) (kN-mm/rad.)	Rotational Stiffness about Y (KRY) (kN-mm/rad.)	Rotational Stiffness about Z (KRZ) (kN-mm/rad.)
35,635.19	64.8	64.8	2.093e+6	1,105e+6	489.5e+6

A gap element is used to model the gap between the superstructure and the substructure, which allows for the possibility of ponding in the longitudinal direction. The initial gap was set to 2 centimeters, as specified in the as-built drawing. The stiffness of the gap element is set to approximately 100 times the axial stiffness of the superstructure to avoid numerical errors.

2.1.3 Substructure

The substructure system of the studied bridges consists of octagonal cross-section reinforced concrete columns with a top slab, illustrated in Figs. 5(a) and (d). The cross-sectional dimension of the columns is 1.60×1.60 m. To accurately capture the inelastic behavior of the bridge structures, the lower portions of the bridge columns are modeled using inelastic elements. For nonlinear static analysis, the inelastic behavior is represented through the application of the lumped hinge technique, specifically employing the lumped axial-bidirectional moment interaction hinge (P-M-M). An

illustrative moment-curvature relationship for the specified column cross-section is displayed in Fig. 5(b). The column reaches its ultimate limit when the extreme fiber of the cross-section attains the ultimate compressive strain. When subjected to an axial load, the moment-curvature response is automatically adjusted to account for the interaction diagram presented in Fig. 5(c).

As a result of a constraint in SAP2000, the plastic hinge length element with a lumped hinge is substituted with a nonlinear spring element with Takeda hysteresis model to represent the inelastic behavior of the bridges during NTHA. The moment-curvature relationships for the column cross-sections of all analyzed bridges, accounting for interaction with axial loads, are incorporated into the nonlinear spring elements within the NTHA model. To ensure consistency in dynamic properties, a comparative assessment is conducted between the fundamental dynamic characteristics of the nonlinear time history analytical model and those of the nonlinear static analytical model.

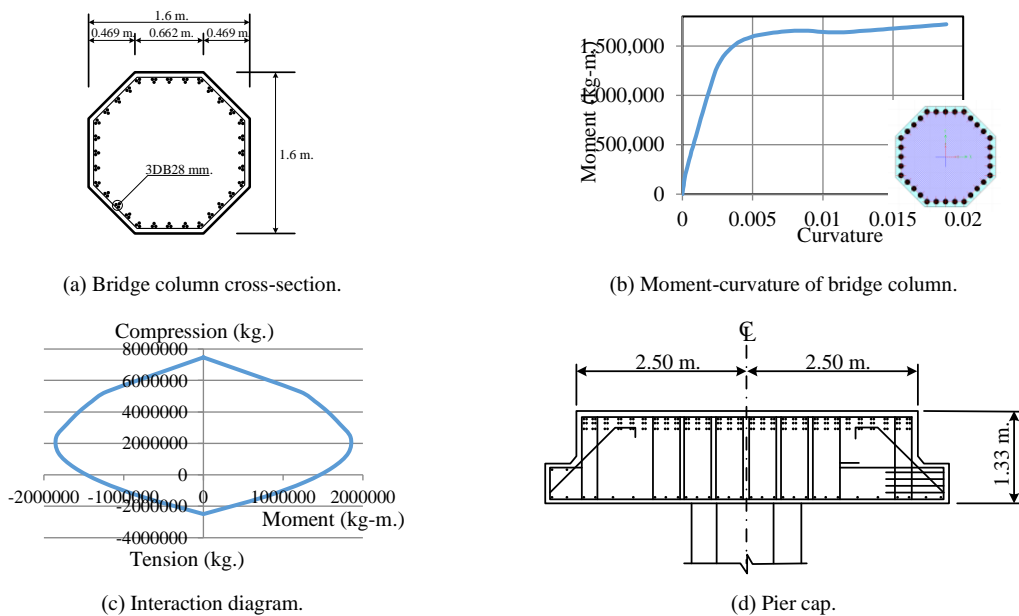


Fig. 5. Details of substructure properties.

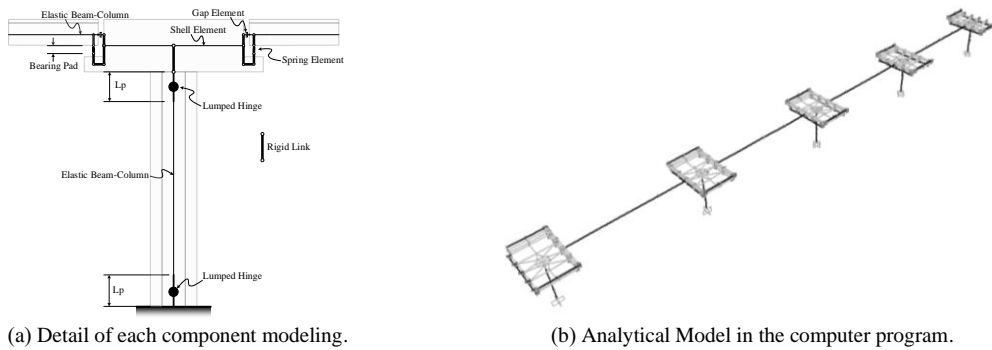


Fig. 6. Analytical model of studied bridges.

The upper part of the column is rigidly joined to a cast-in-place reinforced concrete pier cap, which measures 1.33 meters in thickness, as depicted in Fig. 5(d). This pier cap is represented in the analytical model as an elastic thick shell element. This element is employed to accurately simulate the mass distribution of the pier cap. Due to the substantial thickness relative to its width, a thick element is utilized to properly consider the effects of shear deformation.

2.2 Analytical model of studied bridges

According to the bridge components modeling concept described in Section 2.1, Fig. 6(a) shows a summary of the details. Fig. 6(b) shows the multi-degree-of-freedom (MDOF) analytical model of the studied bridge.

2.3 Dynamic properties of studied bridges

The dynamic characteristics of the studied bridges are assessed using a vibration mode finding analysis method. Eigen-problem analyses are conducted on the analytical model of the bridges to determine the mode shapes and frequencies of all bridges.

The results reveal that the fundamental vibration mode of the single-column bridge is the structural oscillation in a direction perpendicular to the traffic direction, referred to as the transverse direction, while the

oscillation in the same direction as the traffic direction is referred as longitudinal direction. The fundamental mode shapes of the studied bridges in both directions are depicted in Fig. 7. A summary of the dynamic characteristics of these bridges is presented in Table 2.

To verify the analytical model, the computed frequencies for a bridge with a 6.3-meter column height are cross-referenced with those obtained from field test data. In the field test, a typical single-column bridge with the same configuration as the bridge in this study (6.3-meter column height) was investigated. Accelerometers were installed on the top surfaces of both the bridge mid-span and the pier cap. Longitudinal and transverse accelerations were recorded at a sampling rate of 200 Hz. The recorded data was then transformed to the frequency domain to identify the fundamental frequency of the bridge. The frequencies of the bridges in the transverse and longitudinal directions fall within the ranges of 1.60-2.00 Hz and 2.00-2.80 Hz, respectively. The correspondence between the calculated frequencies and the field test results demonstrates that the analytical model falls within the same frequency range as the field measurements. Consequently, the analytical model can be considered a dependable tool for evaluating the seismic performance of these structures.



Fig. 7. Fundamental modes of vibration of the studied bridges in transverse and longitudinal directions.

Table 2. Fundamental dynamic properties of vibration of three studied bridges.

Column Height (m.)	Transverse Direction			Longitudinal Direction		
	Period (sec.)	Frequency (Hz.)	Modal Participating Mass Ratio (%)	Period (sec.)	Frequency (Hz.)	Modal Participating Mass Ratio (%)
4.5	0.450	2.224	53.3	0.272	3.679	66.2
6.3	0.610	1.640	68.3	0.358	2.796	87.1
15.0	1.746	0.573	86.6	0.980	1.020	92.8

The participating mass ratios for all the bridges are additionally presented in Table 2. These findings indicate that, for bridges with taller columns, the fundamental mode governs the vibration characteristics. Conversely, when the column height of the bridge decreases, higher modes can become more significant in influencing the overall vibration behavior.

As outlined in the 2006 Seismic Retrofitting Manual for Highway Bridges by the Federal Highway Administration (FHWA) [32], it is important to account for the presence of concealed cracks in structural members, which can impact the flexural rigidity of these elements. In this study, we have incorporated the consideration of the effect of cracked sections into the seismic performance evaluation process. Consequently, the flexural rigidity of the reinforced concrete columns in all the examined bridges has been reduced to half of the value associated with the gross-section ($0.5E_cI_g$).

3. Seismic Performance Evaluation by Incremental Analysis

Assessing the seismic performance of structures through the incremental analysis concept involves two primary objectives. First, it entails the evaluation of seismic demand under a set of ground motions through

incremental analysis. Second, it encompasses the application of capacity (limit states) to this demand to assess the probabilistic damage potential of the structures.

In this study, the seismic demands of the examined bridges are assessed using Incremental Dynamic Analysis (IDA) and Incremental Static Analysis (ISA). Subsequently, the limit states are determined and superimposed on the demand to investigate the effectiveness of IDA and ISA in evaluating the seismic performance of the studied bridges.

3.1 IDA of multi-degree of freedom system

In conventional IDA, a NTHA is executed using a MDOF analytical model subjected to a set of monotonically increasing ground motions. The aim is to examine the seismic response of the structure under these considered ground motions up to the point of collapse (seismic demand). During this analysis, scalar values representing the intensity of ground motion, known as Intensity Measures (IM), are recorded at each increment of the scaled ground motion. Additionally, the maximum response of the structure called Damage Measure (DM), which can serve as an indicator of the level of damage sustained by the structure, is collected corresponding with IM.

The graphical representation of IM plotted alongside DM is referred to as an incremental dynamic analysis curve (IDA curve). This curve provides insights into the seismic behavior of the structure, covering the entire range from small ground motions to the largest ones capable of causing structural collapse. An overview of the process for conducting IDA for MDOF models of the studied bridges is depicted in Fig. 8. The results from the IDA of MDOF models serve as benchmarks for evaluating the efficiency of the proposed technique in this study.

3.2 IDA of ESDOF based on nonlinear static analysis

The concept of using Nonlinear Static Analysis (NSA) within the Incremental Dynamic Analysis (IDA) framework has been explored to optimize computational efficiency and reduce the time required for Multi-Degree-of-Freedom (MDOF) analysis [14]. The lateral response of the structure is established through

NSA under an appropriate lateral load pattern. In cases where the structures exhibit hysteresis behavior, cyclic nonlinear static analysis is conducted. Subsequently, the derived lateral response is mapped onto a Single Degree of Freedom (SDOF) system to match that of the original MDOF structure. The SDOF's mass is adjusted to ensure that its fundamental dynamic characteristics align with those of the MDOF structure. This equivalent SDOF system, mimicking the lateral behavior of the MDOF system, is employed for the IDA analysis. A visual representation of the Enhanced Single Degree of Freedom (ESDOF) concept can be found in Fig. 9, showcasing how this approach significantly reduces computational time [16].

While an advanced modal IDA method has been proposed [16], it necessitates conducting IDA for each mode separately. In contrast, the method proposed in this study streamlines the process by integrating a single-run analysis of NSA and IDA.

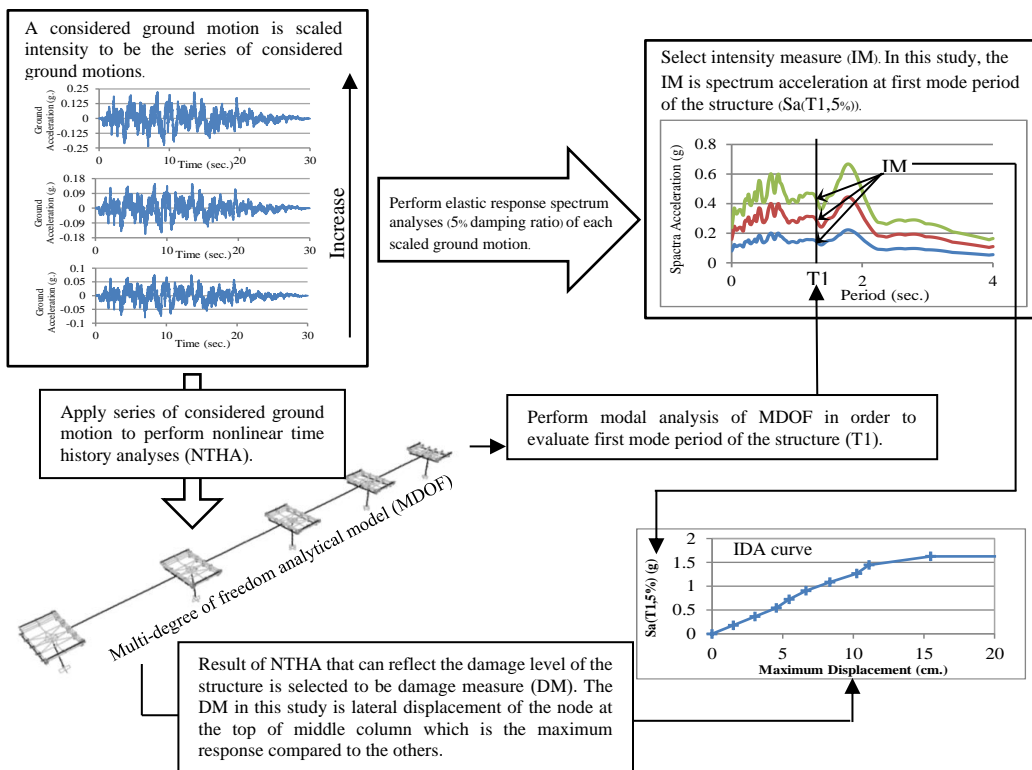


Fig. 8. Concept of incremental dynamic analysis of MDOF single column bridges.

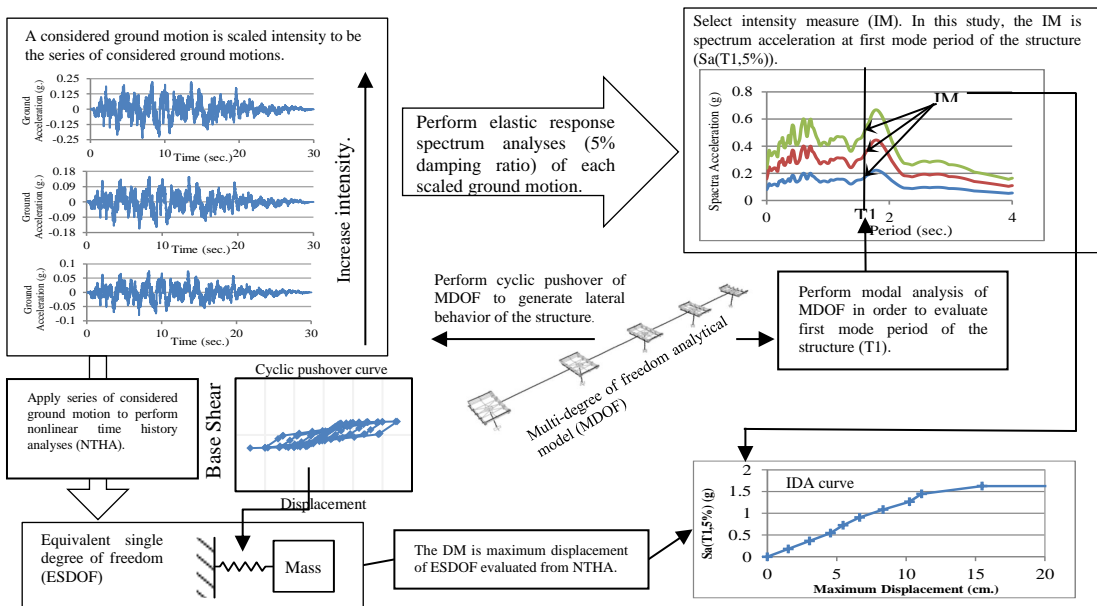


Fig. 9. Concept of incremental dynamic analysis of ESDOF based on nonlinear static analysis.

3.3 Incremental static analysis by incremental capacity spectrum method

The Incremental Static Analysis (ISA) using the Incremental Capacity Spectrum Method (ICSM) combines elements from both the Capacity Spectrum Method (CSM) and incremental analysis. To determine the maximum response for each scaled ground motion considered, the CSM approach was employed, resulting in the DM. These DM values, evaluated for a series of scaled ground motions, are then plotted alongside the corresponding IM to create the Incremental Static Analysis curve (ISA curve). The concept of ICSM is summarized and depicted in Fig. 10.

3.4 Lateral load patterns for single-run nonlinear static analysis

3.4.1 Conventional-based lateral load pattern

When assessing the seismic behavior of structures using NSA based methods, international standards, such as FEMA 356 [33], recommend the consideration of at least two distinct lateral load patterns. These load patterns can be chosen from the following two categories. The first category is the modal pattern. The distribution of vertical load can be selected from one of the following options: a distribution that is proportional to the shape of the fundamental mode in the direction being analyzed, and a distribution that is proportional to the story shear distribution obtained by combining modal responses derived from a response spectrum analysis of the building. This analysis should include an adequate number of modes to encompass at least 90% of the total building mass while considering the appropriate ground motion spectrum.

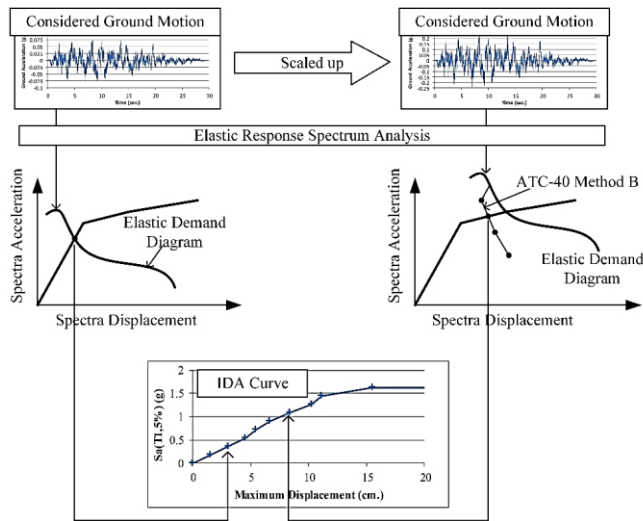


Fig. 10. Concept of Incremental Capacity Spectrum Method (ICSM).

For the second pattern, the distribution can be chosen from the following options: a uniform distribution, which involves lateral forces at each level being proportional to the total mass at each level (or uniform acceleration load distribution), and an adaptive load distribution, which dynamically adjusts as the structure undergoes displacement.

In this study, both of the lateral load patterns, chosen from the two categories mentioned earlier, are employed to examine the impact of various lateral load patterns on the seismic behavior of single-column RC bridges using the IDA of ESDOF concept. The first load pattern distributes the load in proportion to the fundamental mode in the transverse direction and is referred to as the "First mode load pattern (1st)." The second load pattern involves a uniform distribution of lateral forces at each level, which is proportional to the total mass at each level, and is referred to as the "Uniform acceleration load pattern (Unif)."

3.4.2 Proposed multi-modes combination load pattern

A Multi-Modes Combination load pattern (MMC) is introduced in this study to address the influence of higher modes while preserving the simplicity of single-run NSA

and NTHA of ESDOF method. The load distribution is determined by straightforwardly combining mode shapes, each weighted by its respective modal participating mass ratios, as follows:

$$F_j = \sum_{n=1}^N \Gamma_n \phi_{nj}, \quad (3.1)$$

where F_j is the force at the j degree of freedom. Γ_n is the modal participating mass ratio of n mode. And ϕ_{nj} is the mode shape value at j degree of freedom of n mode which are each normalized with respect to the mass matrix such that $\phi_n^T M \phi_n = 1$. N is the number of consideration modes.

The proposed MMC pattern defines the load distribution utilized for conducting displacement-based NSA in this study, using SAP2000 as the tool. The load magnitude is incrementally increased until the monitored point's displacement reaches the specified value, all while maintaining the load distribution proportion as specified. This approach bears similarities to the mode combination method introduced by Kunnath [34] for force-based nonlinear static analysis. However, this study simplifies the methodology by eliminating a few parameters, making it more straightforward while retaining

its accuracy for displacement-based nonlinear static analysis.

Table 3 presents the mode shapes and the corresponding modal participating mass ratios. In the context of the MMC approach employed in this study, a total of four modes, as indicated in Table 3, are combined to encompass at least 80% of the total mass for the studied bridges with short and medium column height. For the studied tall column height bridge, the combination of four lateral modes was also applied.

3.4.3 Comparison of load patterns

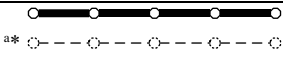
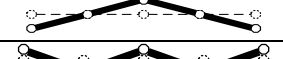
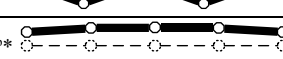
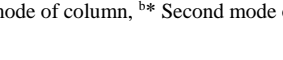
As outlined in sections 3.4.1 and 3.4.2, this study compares the three designated load patterns for the bridge with a column height of 6.3 meters, as depicted in Fig. 11. Which illustrates that the Unif pattern results in the lowest magnitude of resultant force, while the 1st pattern yields the highest magnitude of resultant force. The magnitude of the resultant force produced by the MMC pattern falls between those of Unif and 1st. It's important to note that the discrepancy in node levels between the top slab and the superstructure arises from the modeling approach. Specifically, the 1.33-meter-thick cast-in-place reinforced concrete slab atop the column is represented using a thick shell element positioned in the middle of the slab's thickness, while the superstructure is modeled using elastic beam-column elements at the centroid of the section. Consequently, the superstructure level is higher than that of the top slab of the column, as evidenced in Fig. 11(b).

3.5 Limit states of the studied bridges

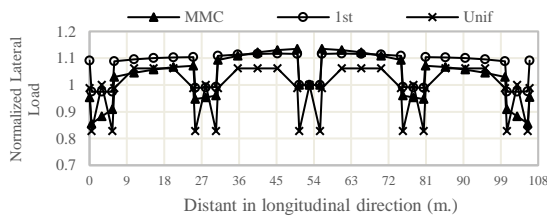
The definition of limit-states holds significance in the assessment of seismic performance using IDA. Various limit-states can be established on the IDA curve. For instance, Vamvatsikos and Cornell [6] applied criteria such as Immediate Occupancy (IO) and Collapse Prevention (CP) limit-states in their IDA analysis of buildings. HAZUS [35] introduces a qualitative definition of limit states known as Damage States (DS) for bridge structures, categorized into five states: none (DS1), minor/slight (DS2), moderate (DS3), major/extensive (DS4), and complete/collapse (DS5) damage states. Mander et al. [7] embrace the DS concept and propose that the quantity of each state can be derived from the pushover curve of a bridge. In the case of older bridge columns, Jeon et al. [27] recommend limit values of 0.5%, 1%, 2%, and 2.5% column drifts (Δ/L) to correspond with Slight, Moderate, Extensive, and Complete damage states, respectively.

The studied bridges are single column reinforced concrete bridge that have been constructed since 1976. In the case of this bridge type, the displacement of the column serves as an indicator of the bridge's damage level. Therefore, for this study, the column displacement is chosen as the engineering demand parameter (EDP). Following the recommendation of Jeon et al. [27], for the studied bridges, the EDP encompasses four distinct limit states, namely: slight, moderate, extensive, and complete damage states.

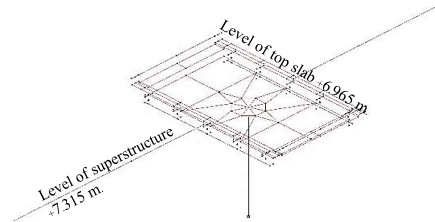
Table 3. Mode shapes and participating mass ratios of three studied bridges in transverse direction for MMC load pattern.

Mode Shape	Participating Mass Ratio (%)		
	4.5 m column height	6.3 m column height	15 m column height
	53.3	68.3	86.6
	0.53	0.62	0.09
	0.12	0.15	0.01
	28.4	15	1

^{a*} First mode of column, ^{b*} Second mode of column.



(a) Comparison of transverse load patterns.

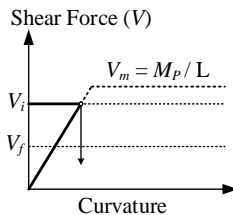


(b) Different level of top slab and superstructure.

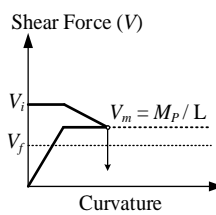
Fig. 11. Comparison of three studied load patterns of the studied bridges with 4 spans and 6.3 m column height (see Fig. 6).

According to FHWA [32], the plastic rotational capacity of a structural member should be determined based on the governing limit state applicable to that member. The governing limit state corresponds to the state with the lowest plastic rotational (or plastic curvature) capacity. Additionally, the failure mechanisms for bridge columns can be categorized into three types: brittle failure (shear failure), semi-ductile failure (flexure to shear failure), and flexural failure, as illustrated in Fig. 12. The shear demands (V_m) for the columns of the studied bridges are

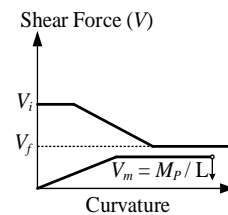
estimated by considering the moment capacity of the cross-section of the bridge column, accounting for the interaction between axial force and bending moments in two axes. These estimated shear demands are then compared to the assessed initial and final shear capacities (V_i and V_f) of the bridge column members to determine the type of failure exhibited by the studied bridges according to FHWA [32]. The results are presented in Table 4, with more comprehensive details available in Chomchuen [36].



(a) Brittle failure



(b) Semi-ductile failure



(c) Flexural failure

Fig. 12. Possible failure mechanisms of bridge column with shear failure consideration according to FHWA [32].

Table 4. Evaluation of failure type of the all studied bridges by comparing shear demands with shear capacities of bridge column members.

	Bridge column height		
	4.5 meters	6.3 meters	15.0 meters
Initial Shear Capacity (V_i) (kg.)	382,483.1	361,768.2	338,731.9
Final Shear Capacity (V_f) (kg.)	316,794.2	296,079.3	273,043
Shear Demand (V_m) (kg.)	412,877.5	296,423.6	124,664.5
Failure type	Brittle	Semi-Ductile	Flexure

Table 5. Limit states of all studied bridges with failure mechanism consideration.

Damage States	Lateral Displacement Limit (cm.) (Column drift, Δ/L (%))		
	4.5 meters column height	6.3 meters column height	15 meters column height
Slight	-	3.48 (0.5)	7.83 (0.5)
Moderate	-	6.97 (1.0)	15.67 (1.0)
Extensive	-	-	31.33 (2.0)
Complete	2.49 (0.48) (Brittle shear failure)	12.75 (1.83) (Semi-ductile failure)	39.16 (2.5) (Flexural Failure)

Table 4 reveals that the bridge with short columns experiences shear failure, which constrains its capacity. The bridge with medium columns can deform into a semi-ductile state, displaying limited plastic deformation. On the other hand, the bridge with tall columns exhibits flexural failure, with the compressive strain of unconfined concrete reaching its ultimate value. The determined failure mechanisms of the studied bridges are considered in conjunction with the previously described limit states in this study. Consequently, the defined limits for each damage state used in this research are summarized in Table 5.

The results presented in Table 5 indicate that the bridge with short columns experiences a brittle shear failure and collapses at only 0.48% drift. The bridge with medium columns undergoes a semi-ductile failure, leading to collapse at 1.83% drift. The collapse of the bridge with tall columns is governed by the limit corresponding to the complete damage state, occurring at a 2.5% drift. It's essential to note that when estimating the cross-sectional capacity based solely on the interaction of axial force and bidirectional moments, the calculated flexural collapse limit exceeds 2.5% drift. This discrepancy arises from the method not automatically and directly accounting for shear failure and column drift limitations.

4. Artificial Ground Motions

This study uses the spectrum match technique for generating 20 artificial ground motions. The target spectrum is a design spectrum for an inner area of Bangkok [37]. The ground motion for the inner area of Bangkok from the design standard is selected to be the prototype. Then, the commercial software SeismoSignal was used to generate the 20 different ground motions from the selected prototype. Response spectra of 20 generated ground motions are compared to the target spectrum in Fig. 13. The generated ground motions are increased time by time and applied to the structures in IDA.

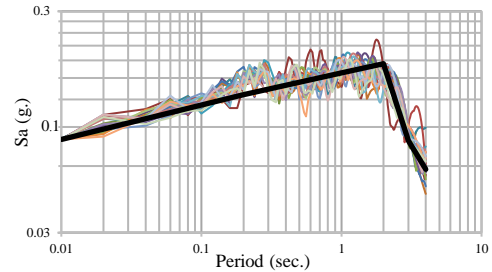


Fig. 13. Comparisons of design spectrum and spectrums of twenty generated ground motions for inner area of Bangkok.

5. Nonlinear Static Analysis of Studied Bridges with Various Load Patterns

To assess the seismic performance of structures using the concept of IDA of ESDOF, the initial step involves deriving the equivalent lateral behavior of ESDOF through NSA of MDOF. Three chosen lateral load patterns, including the proposed load pattern, are applied to the MDOF models of the studied bridges. Subsequently, NSA is conducted on the MDOF models of the studied bridges, and the results are depicted in Fig. 14.

Fig. 14 illustrates a substantial dependency of the lateral behavior of the studied bridges on both the height of the bridge columns and the selected lateral load pattern. As the height of the bridge columns increases, there is a noticeable decrease in the lateral capacities of the studied bridges due to the greater moment arm.

In Fig. 14, it is evident that the utilization of two different load patterns, as per FEMA 356, results in significantly varying lateral capacity and stiffness, particularly notable in the case of bridges with low first-mode participating mass ratios, such as those with short columns (Fig. 14(a)). The maximum base shear capacity of these bridges, evaluated using the 1st, is approximately 62% of those assessed using the Unif, whereas the MMC provides about 93% of the capacity evaluated by Unif. For bridges with medium columns, the maximum capacity assessed with the 1st is around 75% of that obtained with the Unif, while the MMC yields about 94% of the capacity determined with Unif. In the case of

bridges with tall columns, the maximum capacity under the 1st is approximately 88% of that under the Unif, whereas the MMC offers about 95% of the Unif. Additionally, the maximum capacity of the studied bridges with column heights of 4.5 meters, 6.3 meters, and 15 meters, evaluated by MMC when considering only the interaction of axial force and bidirectional moments, corresponds to 52.40%, 38.18%, and 17.06% of their total weights, respectively. When taking into account additional factors such as shear failure and column drift, the maximum base shear capacity of these bridges with respective

column heights becomes 41.43%, 36.81%, and 16.23% of their total weights, respectively.

The following conclusions can be drawn from Fig. 14 and Table 2. 1). The influence of different load patterns diminishes as the bridge column height or the first-mode participating mass ratio of the bridge increases. 2). The proposed MMC load pattern consistently provides more accurate estimates of seismic capacity for all the studied bridges. 3). The Unif load pattern tends to produce upper-bound results, while the 1st" load pattern tends to yield lower-bound results.

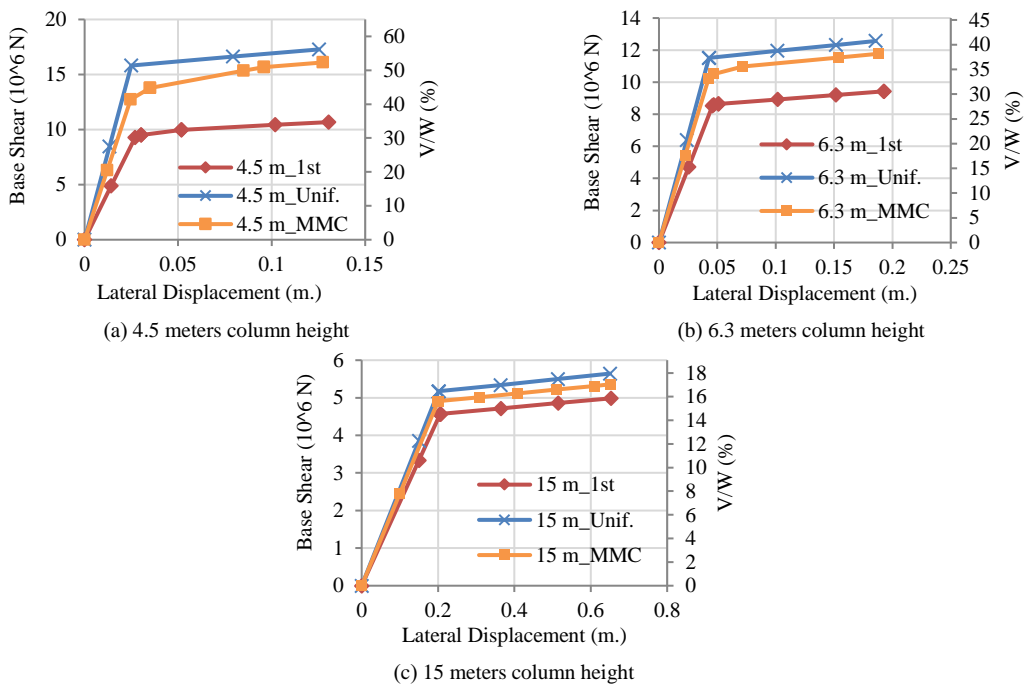


Fig. 14. Lateral capacities of three studied bridges in transverse direction by NSA with three different load patterns.

6. Effects of Hysteresis Model on the IDA curves

To assess the inelastic responses of the structures, it is crucial to model the hysteresis behavior of these structures. This study delves into the impacts of hysteresis models on the IDA curve.

6.1 Hysteresis model

This study examines three pre-defined hysteresis models available in SAP2000. These models, namely the Kinematic model, Pivot model, and Takeda model, are depicted in Figs. 15(a)-(c), respectively. The purpose of considering these three models is to simulate the hysteresis behavior of ESDOFs and observe their impact on the IDA curves for the

studied bridges, which are generated using the ESDOF-based IDA approach.

The Kinematic model is employed to simulate hysteresis behavior without inducing degradation in the hysteretic loop. The Takeda model, on the other hand, is used to model hysteresis behavior with a degrading hysteretic loop, as per the Takeda model. Both models are built-in functions, and the program automatically generates all the necessary parameters. The Pivot model shares similarities with the Takeda model, but it requires additional parameters for controlling the degradation of the hysteretic loop. This model is particularly suitable for simulating the behavior of reinforced concrete members. It is based on the observation that unloading and reverse loading tend to converge toward specific points, referred to as pivot points, in the force-deformation plane [38]. In this study, cyclic nonlinear static analysis (CNSA) of the Multi-Degree-of-Freedom (MDOF) structures is performed to evaluate the parameters required for implementing the Pivot model for all the studied bridges.

Fig. 16 illustrates the comparisons between the cyclic lateral behaviors of the bridge with a 6.3-meter column height, obtained from CNSA of MDOF and CNSA of ESDOF. It is apparent that the ESDOF model with the Kinematic hysteresis model produces an overly exaggerated hysteretic loop, whereas both the ESDOF models with the Pivot and Takeda hysteresis models yield accurate

hysteretic loops when compared to the MDOF results.

6.2 Comparison of IDA curves evaluated by IDA of ESDOF with three different hysteresis models

The IDA curves for the three studied bridges, generated using the IDA of ESDOF with three different hysteresis models, are compared with the IDA curves produced by IDA of MDOF. To facilitate the observation of the effects of different hysteresis models, Fig. 17 displays the IDA curves for the studied bridges under the A1 ground motion. Upon examining the shape and maximum capacity of the IDA curves in Fig. 17, it becomes evident that the IDA curves of ESDOF with the Kinematic hysteresis model exhibit significant differences in maximum capacity when compared to the IDA curves of MDOF. Conversely, ESDOF models employing the Pivot and Takeda hysteresis models provide more accurate results. Notably, the IDA curves of ESDOF with the Takeda model closely align with the IDA curves of MDOF only for bridges with short and medium column heights. In contrast, the IDA curves of ESDOF with the Pivot model demonstrate good agreement with the IDA curves of MDOF across all cases. Consequently, the IDA analysis in this study will be carried out using the ESDOF model with the Pivot hysteresis model.

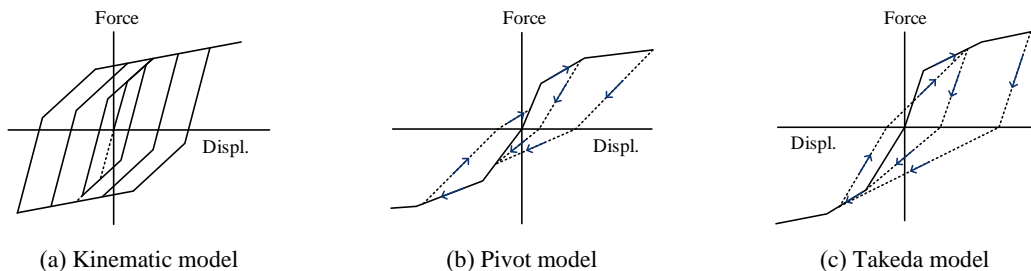


Fig. 15. Three different hysteresis models (modified from CSI [38]).

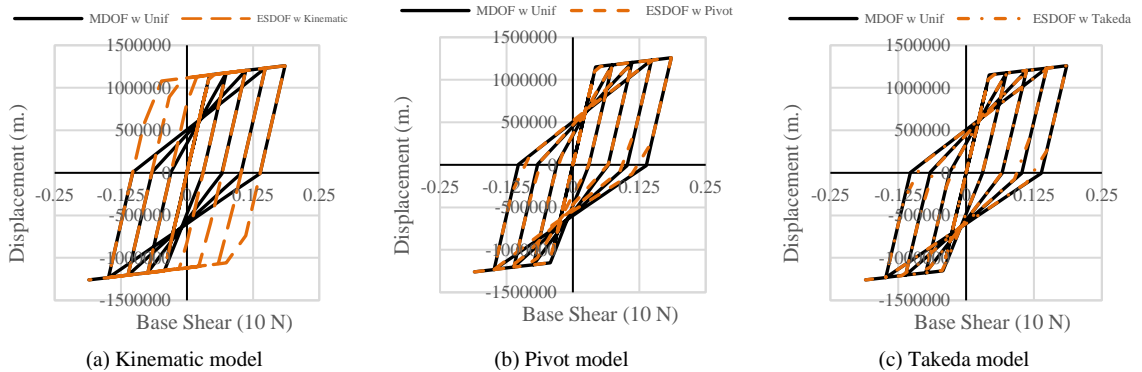


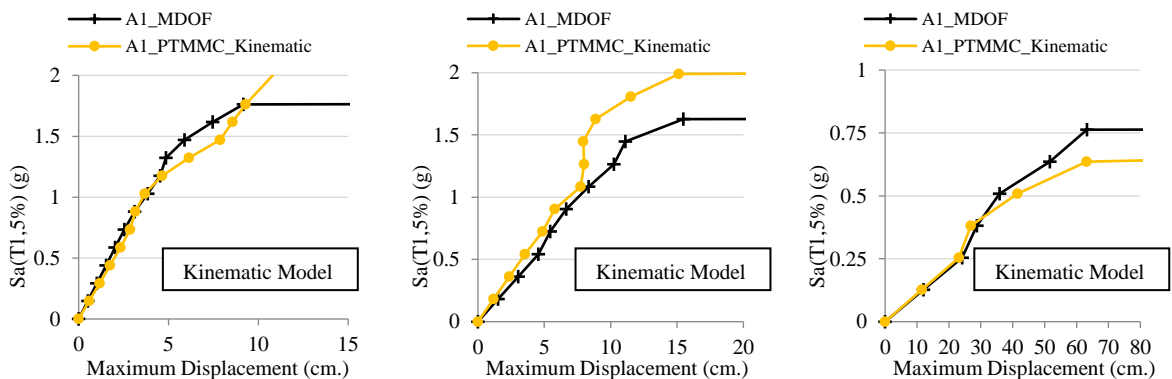
Fig. 16. Comparisons of cyclic lateral behavior of the studied bridge with 6.3 m. column height obtained from CNSA of MDOF and CNSA of ESDOF with three different hysteresis models.

7. Incremental Dynamic Analysis of Studied Bridges by ESDOF with Various Load Patterns

IDA is conducted for the studied bridges using the ESDOF, employing three different load patterns, across 20 artificial ground motions. The purpose of this analysis is to comprehensively explore and elucidate the impact of varying lateral load patterns on the results of IDA of ESDOF.

Figs. 18(a)-(c) depicts IDA curves of the studied bridges with column heights of 4.5 m., 6.3 m., and 15 m., respectively. These IDA curves are generated from the ESDOF, utilizing lateral capacity information derived from the 1st, Unif, and MMC, and are referred to as ESDOF with PT1, ESDOF with PTU, and ESDOF with PTMMC, respectively. The

results exhibit notable variations across 20 artificial ground motions. Therefore, the 16th, 50th, and 84th percentiles are provided. The results reveal that the IDA curves obtained by ESDOF are essentially related to lateral capacity generated by NSA. This implies that IDA curves obtained by ESDOF are significantly influenced by the choice of lateral load patterns. It's worth noting that different load patterns lead to differences in the capacity and stiffness of ESDOF, as previously demonstrated in Fig. 14. Consequently, even when ESDOF models have identical frequency and damping, variations in capacity, mass, and stiffness result in different IDA curves. Thus, the conclusions drawn from IDA with various load patterns of the ESDOF align with those from NSA using different load patterns.



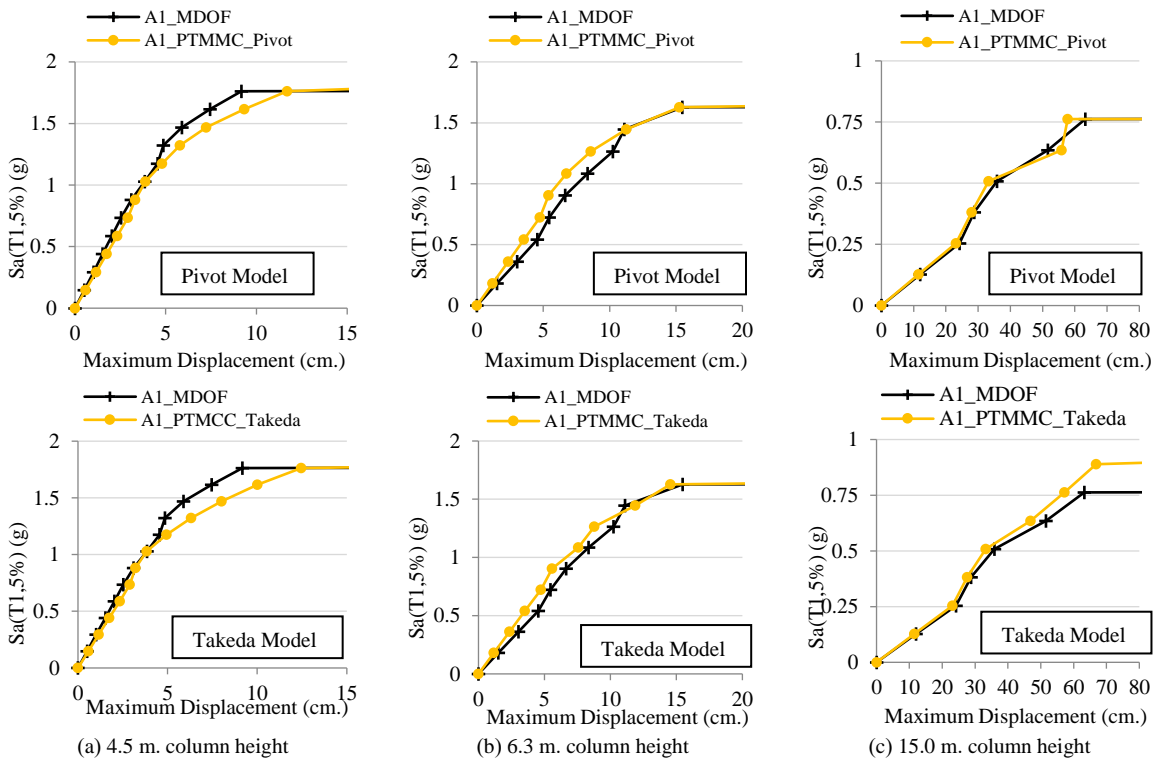


Fig. 17. Comparisons of IDA curves of three studied bridges under A1 artificial ground motions generated by IDA of ESDOF with three different hysteresis models[†]

8. Efficiency of IDA of ESDOF and ISA by ICSM in Evaluating Seismic Performance of the Studied Bridges

8.1 Effects of various lateral load patterns on the IDA and ISA curves

To conveniently investigate the effect of various lateral load patterns on the results of IDA of ESDOF and ISA, the median IDA curves obtained by IDA of ESDOF and ISA curves with three different lateral capacities are compared with those obtained by IDA of MDOF in Figs. 19(a)-(c) for the studied bridges with column heights of 4.5 m., 6.3 m., and 15 m., respectively. The median IDA curves are obtained from applying statistical theory to the results of IDA of ESDOF and MDOF as shown in Fig. 18 for ESDOF. The design spectra for the Bangkok area are used for evaluating the median ISA curves in this study because 20 artificial ground motions

are generated corresponding to those design spectra as described in section 4.

The comparisons depicted in Figs. 19(a)-(c) highlight the significant impact of lateral load pattern selection on the outcomes of both IDA of ESDOF and ISA. The influence of different lateral load patterns becomes particularly evident when the bridge has a low first-mode participating mass ratio, as indicated in Table 2.

Fig. 19 reveals that conducting IDA of ESDOF with the 1st mode load pattern leads to a significant underestimation of seismic capacity, while the Unif load pattern results in a slight overestimation of seismic capacity, especially when compared to the results obtained from IDA of MDOF for the bridges with 4.5 m column heights. as depicted in Fig. 19(a). The influence of the load pattern diminishes as the first-mode participation mass ratio of the bridge increases, as evidenced in

Figs. 19(b) and (c) for bridges with 6.3 m. and 15 m. column heights, respectively.

The ISA curves are affected by various lateral load patterns in the same way as IDA curves of ESOE. However, Figs. 19(a)-(b) also shows that the ISA curves by ICSM with lateral capacities obtained from all studied lateral load patterns, i.e., uniform acceleration load pattern (CSM_PTU), 1st mode load pattern (CSM_PT1), and MMC load pattern (CSM_PTMMC), result in significantly under-estimating seismic capacities of studied bridges with 4.5m. and 6.3 m. column height. Unlike Figs. 19(a)-(b), Fig. 19(c) shows that the ICSM of a studied bridge with 15 m. column height agrees well results with IDA of MDOF for all studied lateral load patterns.

8.2 Efficiency of IDA of ESDOF with various load patterns

The intensity measurements (IM) at each damage state of the studied bridges are examined from Fig. 19 and summarized in Table 6 and Table 7 for IDA of ESDOF and ISA, respectively, in order to investigate the efficiency of both methods with different load patterns for evaluating the seismic performance of the studied bridges.

The results in Table 6 show that the median IMs at collapse of the studied bridge with 4.5 m. column height evaluated by ESDOF with PT1, PTU, and PTMMC are 62.3%, 118.9%, and 94.5% of those evaluated by MDOF, respectively. For the studied bridge with 6.3 m. column height, the median IMs at collapse evaluated by ESDOF with PT1, PTU, and PTMMC are 79.9%, 107.8%, and 98.7% of those evaluated by MDOF, respectively. For the studied bridge with 15 m. column height, the median IMs at collapse evaluated by ESDOF with PT1, PTU, and PTMMC are 109.5%, 113.9%, and 108.7% of those evaluated by MDOF, respectively.

The comparative results in Table 6 show that ESDOF with PT1 and PTU give the acceptable results only for the bridge with tall column while the ESDOF with PTMMC gives the acceptable results for all case studies compared with MDOF. Therefore, it can be concluded that the proposed MMC results in the most accurate median IM for all damage states of all studied bridges compared with other conventional load patterns for single-run analysis. Moreover, using IDA of ESDOF for evaluating the seismic performance of the studied bridges can reduce the computational time from 60 minutes per load case of MDOF to 4 minutes per load case of ESDOF. That is a reduction of about 93% of computational time.

8.3 Efficiency of ISA by ICSM

Evaluated by ICSM with PT1, PTU, and PTMMC, the results in Table 7 show that the median IMs at collapse of the studied bridge with 4.5 m. column height are 50.8%, 79%, and 96.5% of those evaluated by MDOF, respectively. For the studied bridge with 6.3 m. column height, the median IMs at collapse evaluated by ICSM with PT1, PTU, and PTMMC are 52%, 70.4%, and 72.4% of those evaluated by MDOF, respectively. For the studied bridge with 15 m. column height, the median IMs at collapse evaluated by ICSM with PT1, PTU, and PTMMC are 118.9%, 118.9%, and 119.3% of those evaluated by MDOF, respectively. The results in Table 7 also show that, even if the ICSM uses significantly less computational effort than IDA of MDOF, this method results in significantly under-estimated capacities of studied bridges with 4.5 m. and 6.3 m. column heights and leads to acceptable results only for the studied bridge with high first-mode participating mass ratio, i.e., 15 m. column height in this study.

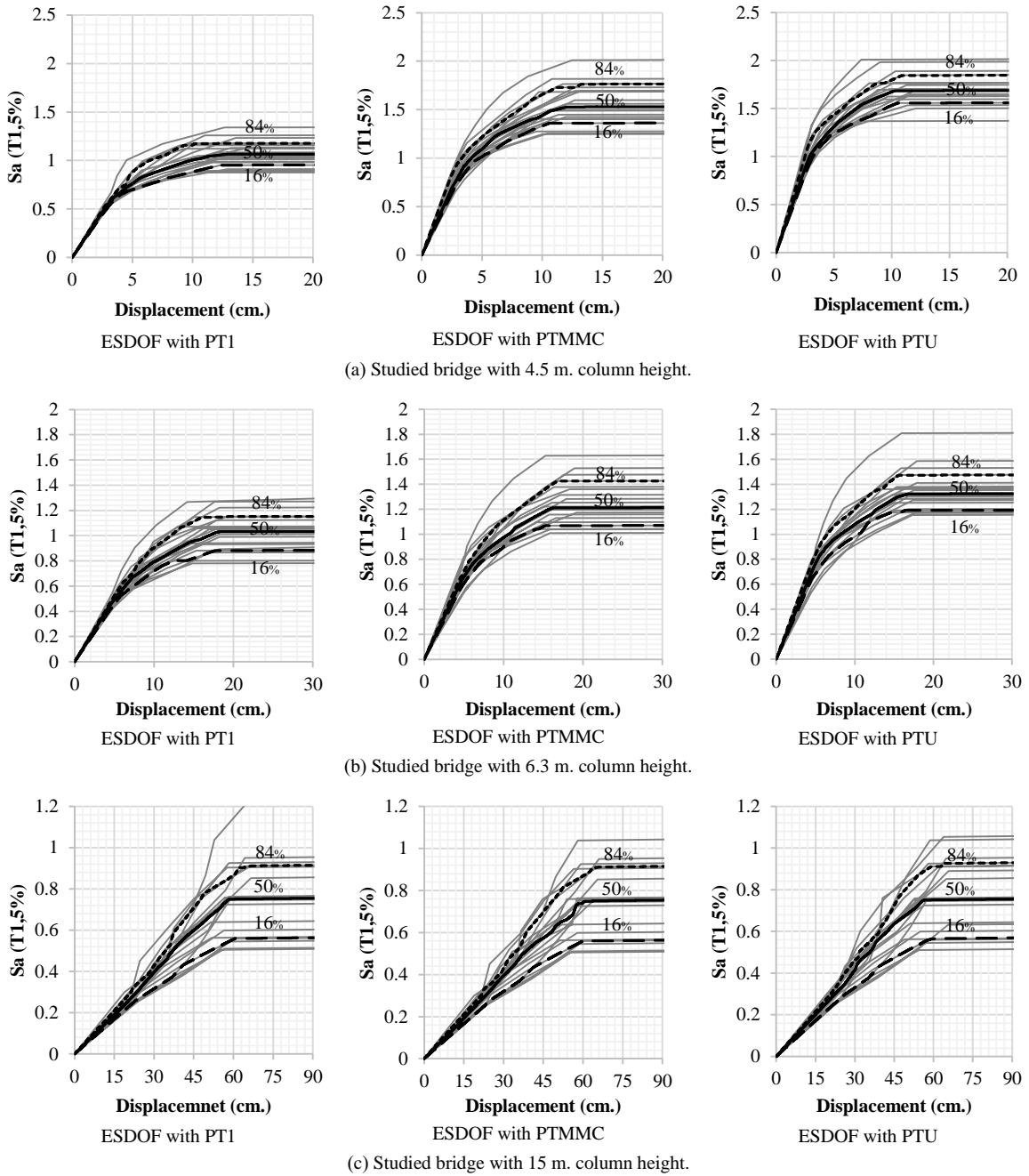


Fig. 18. Incremental dynamic analysis curves by ESDOF of three studied bridges with three different load patterns.

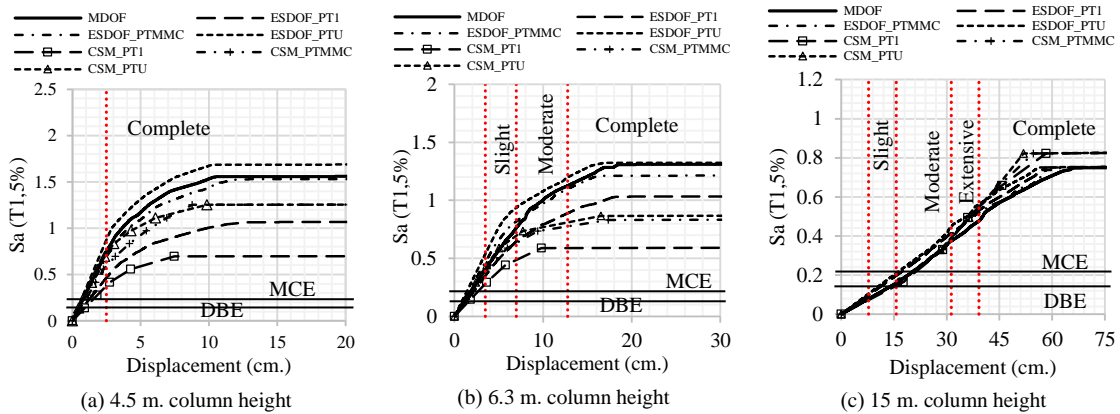


Fig. 19. Comparison of median IDA curves resulted from NTHA of MDOF, NTHA of ESDOF, and ISA by ICSM with three various lateral capacities of three studied bridges, and performance evaluation with shear failure consideration.

Table 6. Comparison of median IMs and standard deviations at each damage state of the studied bridges evaluated from IDA of MDOF and IDA of ESDOF with three different load patterns.

Damage States	4.5 m. column height				6.3 m. column height				15 m. column height			
	MDOF	ESDOF with PT1	ESDOF with PTMMC	ESDOF with PTU	MDOF	ESDOF with PT1	ESDOF with PTMMC	ESDOF with PTU	MDOF	ESDOF with PT1	ESDOF with PTMMC	ESDOF with PTU
Slight	Median IM (g.)	-	-	-	0.403 (100%)	0.346 (85.9%)	0.466 (115.6%)	0.537 (133.3%)	0.079 (100%)	0.099 (125.3%)	0.099 (125.3%)	0.103 (130.4%)
	Standard Deviation	-	-	-	0.029 (100%)	0.068 (234.5%)	0.107 (369%)	0.105 (362.1%)	0.026 (100%)	0.102 (392.3%)	0.104 (400%)	0.098 (376.9%)
	Median IM (g.)	-	-	-	0.766 (100%)	0.646 (84.3%)	0.828 (108.1%)	0.931 (121.5%)	0.161 (100%)	0.198 (123.0%)	0.199 (123.6%)	0.206 (127.9%)
Moderate	Standard Deviation	-	-	-	0.077 (100%)	0.097 (126%)	0.114 (148.1%)	0.116 (150.6%)	0.034 (100%)	0.106 (311.8%)	0.105 (308.8%)	0.100 (294.1%)
	Median IM (g.)	-	-	-	-	-	-	-	0.366 (100%)	0.402 (109.8%)	0.404 (110.4%)	0.427 (116.7%)
	Standard Deviation	-	-	-	-	-	-	-	0.137 (100%)	0.151 (110.2%)	0.147 (107.3%)	0.164 (119.7%)
Extensive	Median IM (g.)	0.746 (100%)	0.465 (62.3%)	0.705 (94.5%)	0.887 (118.9%)	1.130 (100%)	0.903 (79.9%)	1.115 (98.7%)	1.218 (107.8%)	0.461 (100%)	0.505 (109.5%)	0.501 (108.7%)
	Standard Deviation	0.036 (100%)	0.053 (147.2%)	0.118 (327.8%)	0.096 (266.7%)	0.139 (100%)	0.134 (96.4%)	0.119 (85.6%)	0.114 (82%)	0.166 (100%)	0.181 (109%)	0.175 (105.4%)
	Median IM (g.)	-	-	-	-	-	-	-	-	-	-	-
Complete	Standard Deviation	-	-	-	-	-	-	-	-	-	-	-
	Median IM (g.)	-	-	-	-	-	-	-	-	-	-	-
	Standard Deviation	-	-	-	-	-	-	-	-	-	-	-

The results in Table 6 also show that the IMs of MDOF at collapse are 0.746g, 1.130g, and 0.461g for the studied bridges with column heights 4.5 m., 6.3 m., and 15 m., respectively. These correspond to peak ground acceleration of 0.316g, 0.553g, and 0.237g for bridge with 4.5 m., 6.3 m., and 15 m. column heights, respectively.

It should be noted that the studied bridges with short and medium column heights experience collapse due to brittle shear failure and semi-ductile failure, particularly when the shear failure criteria are taken into account (as shown in Table 5). In essence, assessing the seismic performance of these studied bridges through IDA without factoring in shear failure and column drift limitations leads to a

moderate to significant overestimation of their capacity.

In addition, when we compare the obtained IDA curves with design basis earthquake (DBE) and maximum considered earthquake (MCE) for inner area of Bangkok as presented in Figs. 12 and 18, the results indicate that no damage is observed for the bridges with 4.5 m. and 6.3 m. column heights. However, slight damage occurs for the bridge with 15 m. column height under DBE while moderate damage is observed under MCE.

9. Fragility Curves of Studied Bridges

Seismic vulnerability assessments for structures are typically established using probabilistic analyses and are presented in the

form of fragility curves. Seismic fragility provides the probability that a structure or its structural components will reach or surpass a certain damage level during ground motions of a specific intensity. Consequently, fragility curves are employed to probabilistically estimate the extent of damage a structure may experience during an earthquake.

Analytical fragility curves in this study are developed through the process described by Baker [39] and denoted as “Method A” by Porter et al. [40]. A lognormal cumulative distribution function used to define fragility function is shown in Eq. 9.1. Fragility function parameters are evaluated from the results of IDA by taking logarithms of each IDA curve and computing their mean and standard deviation by Eqs. 9.2 and 9.3, respectively.

$$P[DS|IM = S_a(T_1, 5\%)] = \Phi\left(\frac{\ln(IM/\theta)}{\beta}\right), \quad (9.1)$$

$$\ln \theta = \frac{1}{n} \sum_{i=1}^n \ln IM_i, \quad (9.2)$$

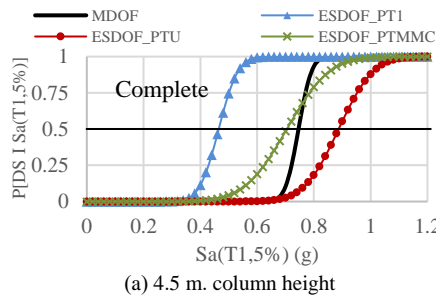
$$\beta = \sqrt{\frac{1}{n-1} \sum_{i=1}^n \left(\ln(IM_i/\theta)\right)^2}, \quad (9.3)$$

where $P[DS|IM = S_a(T_1, 5\%)]$ is the probability that a ground motion with IM will cause the structure to DS , $\Phi(\)$ is the standard normal cumulative distribution function, n is the number of considered ground motions, IM_i is the IM value associated with onset of DS for the i th ground motion, $\ln \theta$ is the mean, and β is the standard deviation.

9.1 Fragility curves by IDA of ESDOF

Figs. 20(a)-(c) show the comparison of fragility curves of the studied bridges by IDA of ESDOF across multiple damage states. The fragility function parameters evaluated in this study are also concluded in Table 6 in order to investigate the efficiency of IDA of ESDOF with various load patterns in evaluating seismic fragility curve. Focusing on only median IM, which is typically defined as the IM associated with a 50% probability of exceeding a damage state, ESDOF with PT1 and PTU give the acceptable value only for the bridge with tall column while the ESDOF with PTMMC gives the acceptable value for all case studies compared with MDOF. However, the dispersions of the results obtained by IDA of ESDOF are significantly different from those by IDA of MDOF, especially for slight and moderate damage states. The IDA of ESDOF gives more widely spread IDA curves than IDA curves of MDOF.

By IDA curve of MDOF, the results also show that IM in terms of spectrum acceleration of the bridge with 4.5 m. column height at 16%, 50%, and 84% probability of collapse are equal to 0.710g, 0.746g, and 0.782g, respectively. For the bridge with 6.3 m. column height, the IM at 16%, 50%, and 84% probability of collapse are equal to 0.993g, 1.130g, and 1.268g, respectively. For the bridge with 15 m. column height, the IM at 16%, 50%, and 84% probability of collapse are equal to 0.105g, 0.461g, and 0.627g, respectively.



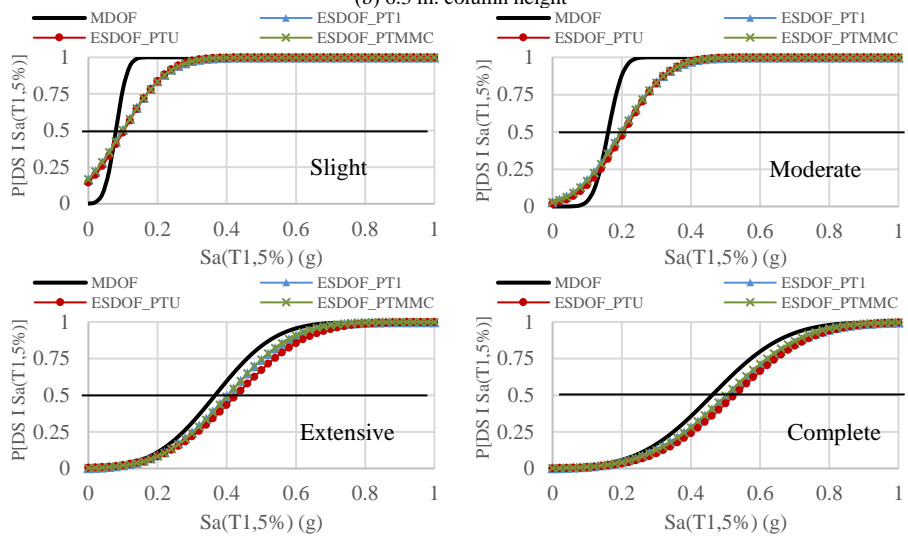
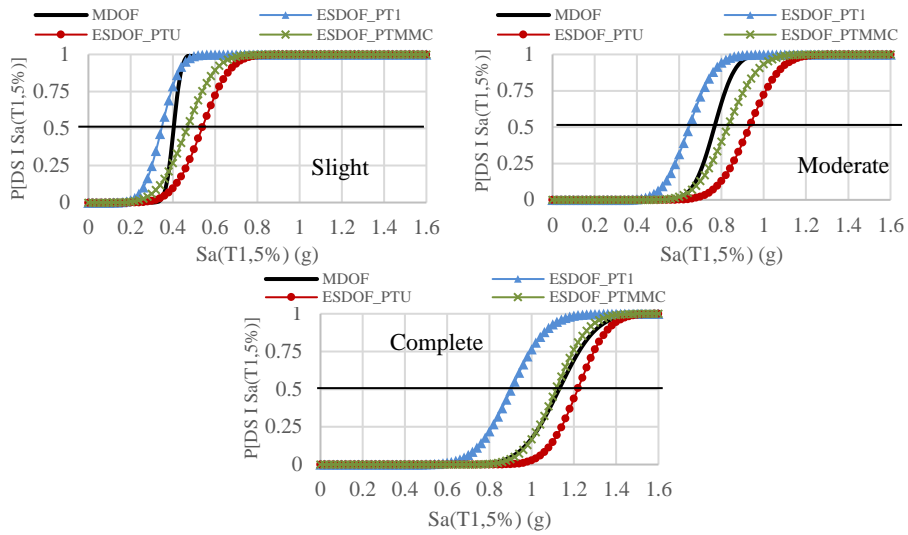
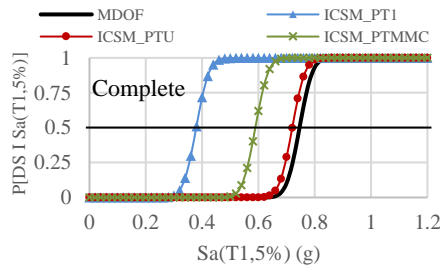


Fig. 20. Comparison of fragility curves of three studied bridges generated from MDOF and ESDOF with three various lateral load patterns.



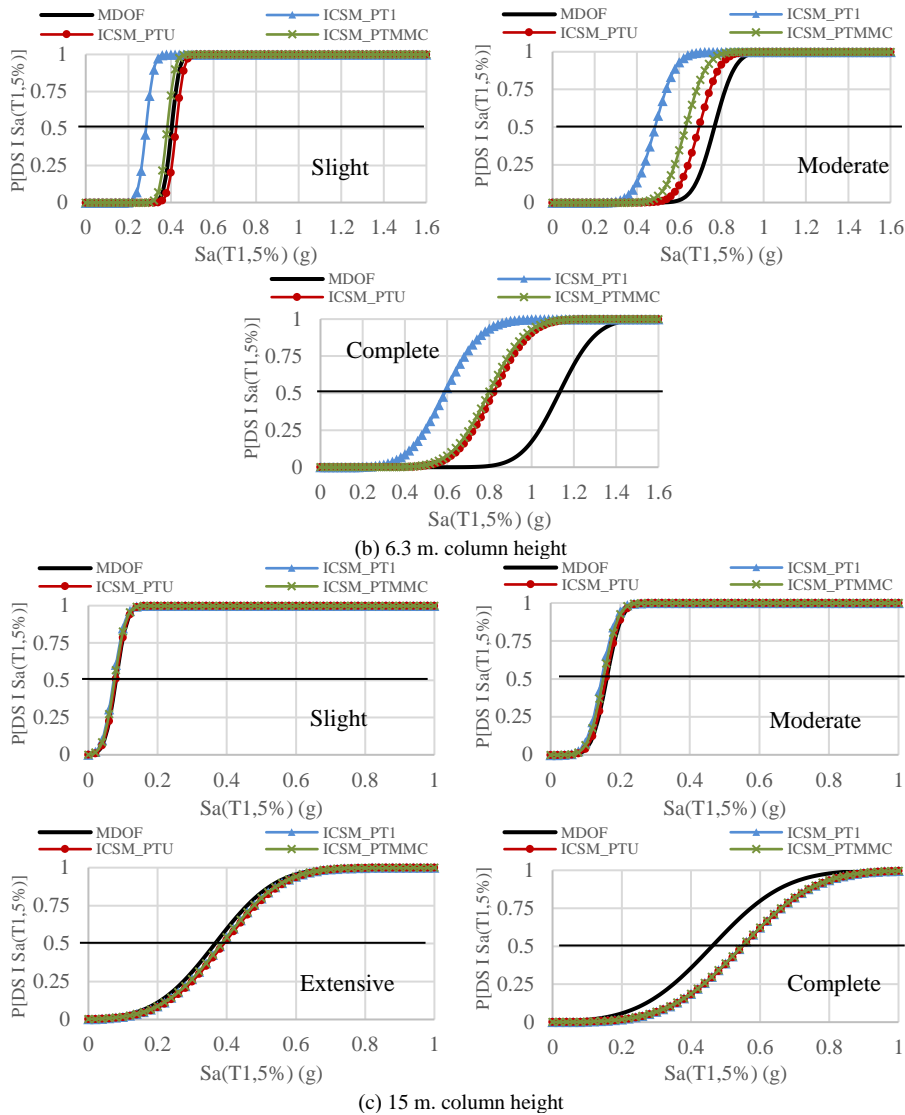


Fig. 21. Comparison of fragility curves of three studied bridges generated from MDOF and ICSM with three various lateral load patterns.

9.2. Fragility curves by ISA by ICSM

The design spectrums for Bangkok area are used to evaluate the median ISA curves under three different load patterns. Median IMs of each limit state are evaluated by combining the capacity limit states to the generated demands resulted in Table 7. However, standard deviations of data are also required in order to generate the fragility curve. There are several suggestions of dispersion values for limit states with unknown dispersions, e.g. FEMA 350 [41] and

Nielson and DesRoches [43]. However, Mander et al. [7] shows that the dispersions vary depending on the level of IM. Therefore, the dispersions of each limit state of the studied bridges obtained from IDA of MDOF as shown in Table 6 are applied for generating fragility curves of ISA by ICSM in this study. Figs. 21(a)-(c) show the comparison of fragility curves of ISA by ICSM and IDA of MDOF of the studied bridges across multiple damage states.

The results in Fig. 21 emphasize that, even if the ISA by ICSM uses significantly less computational effort than IDA of MDOF, this method results in significantly underestimated capacities of studied bridges with 4.5 m. and 6.3 m. column heights and leads to acceptable results only for the studied bridge with high first-mode participating mass ratio, i.e., 15 m. column height in this study.

10. Conclusion

This study intensively investigates applicability of IDA of ESDOF and ISA by ICSM for evaluating the seismic performance of three studied bridges under 20 artificial ground motions. The efficiency of the proposed techniques is also thoroughly examined, and the results give rise to the following conclusions.

- Utilizing the concept of ESDOF for seismic performance evaluation of the studied bridges through IDA substantially reduces computational time, IDA of ESOF is about 15 time faster than IDA of MDOF for analysis the structure under each load case. This amounts to an impressive 93% reduction in computational time.

- The distinct load patterns lead to variations in the capacity and stiffness of the ESDOF. Consequently, despite having identical frequency and damping characteristics, the disparities in capacity, mass, and stiffness among the ESDOF result in different IDA curves. The ESDOF with the proposed multi-modes combination load pattern, utilizing a single-run of NSA and IDA, yields better accuracy in assessing seismic performance compared to conventional load patterns for all the studied bridges, compared with IDA of MDOF.

- Either the first mode or the uniform acceleration lateral load patterns, as per FEMA 356, can be efficiently employed when implementing the concept of ESDOF for evaluating the seismic performance of the studied bridges. This is particularly applicable when the first-mode participating mass ratio

exceeds 80% of the total mass, as is the case for the 15-meter column height in this study.

- In terms of the seismic performance of the studied bridges with a first-mode participating mass ratio less than 80% of the total mass, such as the cases for the 4.5 meters and 6.3 meters column heights in this study, it is observed that the ESDOF employing the first mode load pattern tends to moderately underestimate capacities. Conversely, the uniform acceleration load pattern yields a slight overestimation of capacities.

- The studied bridges with short and medium column heights experience collapse due to brittle shear failure and semi-ductile failure when the shear failure criteria are taken into account. In essence, assessing the seismic performance of these studied bridges through IDA without factoring in shear failure and column drift limitations leads to a moderate to significant overestimation of their capacity.

- The IDA curves of ESDOF with kinematic model exhibit significantly different maximum capacity when compared to the IDA of MDOF. In contrast, the ESDOF with the pivot and Takeda hysteresis models yield more accurate results. Specifically, the ESDOF with the pivot hysteresis model demonstrates the highest level of accuracy in generating IDA curves compared to the IDA of MDOF in this study. However, it's important to note that the necessary input parameters for modeling the pivot hysteresis must be extracted from the results of cyclic nonlinear static analysis. Conversely, the ESDOF with the Takeda hysteresis model produces slightly less accurate IDA curves compared to those of the ESDOF with the pivot hysteresis model when compared to the IDA of MDOF. However, it's worth highlighting that the essential parameters for modeling the Takeda hysteresis are automatically generated by the program.

- By using the ISA by ICSM, the interpretation of the huge results of IDA of MDOF is eliminated. The seismic performance can be evaluated by combining the capacity diagram with the demand diagram. The ISA curves can be simply

created from the seismic response of the structure under each level of considered ground motion. The NTHA is not required in this method. Even if the ISA by ICSM uses significantly less computational effort than IDA of MDOF, this method results in significantly under-estimated capacities of studied bridges with 4.5 m. and 6.3 m. column heights and leads to acceptable results only for the studied bridge with high first-mode participating mass ratio, i.e., 15 m. column height in this study.

- The median IMs in term of spectrum acceleration of MDOF at collapse are 0.746g, 1.130g, and 0.461g for the studied bridges with 4.5 m., 6.3 m., and 15 m. column heights, respectively. These correspond to peak ground acceleration of 0.316g, 0.553g, and 0.237g for bridge with 4.5 m., 6.3 m., and 15 m. column heights, respectively.

Acknowledgments

The research described in this paper has been extensively extended from the previous research that was financially supported by the Thailand Research Fund (TRF) under the Royal Golden Jubilee Ph.D. Program and by the Higher Education Research Promotion and National Research University Project of Thailand, Office of the Higher Education Commission.

References

- [1] Applied Technology Council (ATC). Seismic Evaluation and Retrofit of Concrete Buildings (ATC-40). 1996.
- [2] Krawinkler H. and Seneviratna G. D. P. K. Pros and cons of a pushover analysis of seismic performance evaluation. *Engineering Structures*. 1998;20(4-6):452-64.
- [3] Chopra A.K. and Goel R.K. Capacity-demand-diagram methods for estimating seismic deformation of inelastic structures: SDF systems (PEER1999/02). Pacific Earthquake Engineering Research Center: University of California Berkeley, C.A.: 1999.
- [4] Chopra A.K. and Goel R.K. A modal pushover analysis procedure to estimate seismic demands for buildings (PEER2001/03). Pacific Earthquake Engineering Research Center: University of California Berkeley, C.A.: 2001.
- [5] Fajfar P. Capacity spectrum method based on inelastic demand spectra. *Earthquake Engineering & Structural Dynamics*. 1999;28:979-93.
- [6] Vamvatsikos D. and Cornell C.A. Incremental dynamic analysis. *Earthquake Engineering & Structural Dynamics*. 2002;31:491-514.
- [7] Mander J.B. Dhakal R.P. Mashiko N. and Solberg K.M. Incremental dynamic analysis applied to seismic financial risk assessment of bridges. *Engineering Structures*. 2007;29:2662-72.
- [8] Vejdani-Noghreiyani H.R. and Shooshtari A. Comparison of exact IDA and approximate MPA-based IDA for reinforced concrete frames. *Proceedings of the 14th World Conference on Earthquake Engineering*, Beijing, October 2008.
- [9] Tehrani P. and Mitchell D. Seismic performance assessment of bridges in montreal using incremental dynamic analysis. *Proceedings of the 15th World Conference on Earthquake Engineering*, Lisbon, September 2012.
- [10] Tehrani P. and Mitchell D. Seismic response of bridges subjected to different earthquake types using IDA. *Journal of Earthquake Engineering*. 2013;17:423-48.
- [11] Alembagheri M. and Ghaemian M. Damage assessment of a concrete arch dam through nonlinear incremental dynamic analysis. *Soil Dynamics and Earthquake Engineering*. 2013;44:127-37.
- [12] Nazari Y.R. and Bargi Kh. Seismic performance assessment of a two span

- bridge by applying incremental dynamic analysis. *Asian Journal of Civil Engineering*. 2014;15(1):1-8.
- [13] Dolsek M. and Fajfar P. IN2-A Simple alternative for ida. *Proceedings of the 13th World Conference on Earthquake Engineering*, Vancouver, Canada 2013.
- [14] Vamvatsikos D. and Cornell C.A. Seismic Performance, Capacity and Reliability of Structures as Seen through Incremental Dynamic Analysis. Report No. 151; 2005.
- [15] Mofid M. Zarfam P. and Fard B.R. On the modal incremental dynamic analysis. *The Structural Design of Tall and Special Buildings*. 2005;14(4):315-29.
- [16] Han S.W. and Chopra A.K. Approximate incremental dynamic analysis using modal pushover analysis procedure. *Earthquake Engineering and Structural Dynamics*. 2006;35:1853-73.
- [17] Han S.W. Moon K.H. and Chopra A.K. Application of MPA to estimate probability of collapse of structures. *Earthquake Engineering and Structural Dynamics*. 2010;39:1259-78.
- [18] Zarfam P. and Mofid M. On the modal incremental dynamic analysis of reinforced concrete structures, using a trilinear idealization model. *Engineering Structures*. 2011;33:1117-22.
- [19] Chomchuen P and Boonyapinyo V. Incremental dynamic analysis with multi-modes for seismic performance evaluation of RC bridges, *Engineering Structures*. 2017;132:29-43.
- [20] Vielma JC, Porcu MC, and López N. Intensity Measure Based on a Smooth Inelastic Peak Period for a More Effective Incremental Dynamic Analysis. *Applied Sciences*. 2020;10(23):8632.
- [21] Singh G. Fragility Assessment of RC Structure using Incremental Dynamic Analysis Considering Variability of Ground Motion, Damping and Soil Parameters [Master Thesis]. Mumbai: Homi Bhabha National Institute; 2021.
- [22] Miari M and Jankowski R. Incremental dynamic analysis and fragility assessment of buildings founded on different soil types experiencing structural pounding during earthquakes, *Engineering Structures*. 2022; 252:113-8.
- [23] Qu J and Pan C. Incremental Dynamic Analysis Considering Main Aftershock of Structures Based on the Correlation of Maximum and Residual Inter-Story Drift Ratios. *Applied Sciences*. 2022;12(4):2042.
- [24] Felice G.D. and Giannini R. An efficient approach for seismic fragility assessment with application to old reinforced concrete bridges. *Journal of Earthquake Engineering* 2010;14(2):231-51.
- [25] Akbari R. Seismic fragility analysis of reinforced concrete continuous span bridges with irregular configuration. *Structure and Infrastructure Engineering: Maintenance, Management, Life-Cycle Design and Performance*. 2012;8(9):873-89.
- [26] Sadan O.B. Petrini L. and Calvi G.M. Direct displacement-based seismic assessment procedure for multi-span reinforced concrete bridges with single-column piers. *Earthquake Engineering & Structural Dynamics*. 2013;42:1031-51.
- [27] Jeon J.S. Shafieezadeh A. Lee D.H. Choi E. and DesRoches R. Damage assessment of older highway bridges subjected to three-dimensional ground motions: Characterization of shear-axial force interaction on seismic fragilities. *Engineering Structures*. 2015;87:47-57.
- [28] Aviram A. Mackie K.R. and Stojadinovic B. Guidelines for nonlinear analysis of bridge structures in california (PEER2008/03). Pacific Earthquake Engineering Research Center: University of California Berkeley; 2008.
- [29] Yazdani N. Eddy S. and Cai C.S. Effect of bearing pads on precast prestressed concrete

- bridges. *Journal of Bridge Engineering*. 2000;5(3):224-32.
- [30] Thammasat University Research and Consultancy Institute (TU-RAC). *Inspection and Methodology for Replacing Bearing Pads of Expressway in Thailand*. Pathumthani, Thailand. 2007. (in Thai).
- [31] American Association of State Highway and Transportation Officials (AASHTO). *LRFD bridge design specifications*. 5th Edition, Washington, DC, USA. 2010.
- [32] Federal Highway Administration (FHWA). *Seismic retrofitting manual for highway structures: part 1-bridges*. Buffalo, NY, USA. 2006.
- [33] Federal Emergency Management Agency (FEMA). *Prestandard and commentary for the seismic rehabilitation of buildings (FEMA 356)*. Washington, DC, USA. 2000.
- [34] Kunnath S.K. Identification of modal combinations for nonlinear static analysis of building structures. *Computer-Aided Civil and Infrastructure Engineering*. 2004;19:282-95.
- [35] Hazus. *Hazus-MH 2.1 Technical Manual*. Washington, DC, USA. 2003.
- [36] Chomchuen P. *Seismic performance evaluation and improvement of regular reinforced concrete bridges [Ph.D. thesis]*. Pathumthani: Thammasat University; 2015.
- [37] Department of Public Works and Town & Country Planning (DPT). *Seismic resistance design standard (DPT-1302-52)*. Bangkok, Thailand. 2009. (in Thai).
- [38] Computers & Structures (CSI). *SAP2000 analysis reference*. Berkeley, CA, USA. 2011.
- [39] Baker J. W. Efficient analytical fragility function fitting using dynamic structural analysis. *Earthquake Spectra*. 2015;31(1):579-99.
- [40] Porter K. Kennedy R. and Bachman R. Creating fragility function for performance-based earthquake engineering. *Earthquake Spectra*. 2007; 23(2): 471-89.
- [41] Federal Emergency Management Agency (FEMA). *Recommended seismic design criteria for new steel moment-frame building (FEMA 350)*. Washington, DC, USA. 2000.
- [42] Nielson B.G. and DesRoches R. Seismic fragility methodology for highway bridges using component level approach. *Earthquake Engineering & Structural Dynamics*. 2007; 36(6): 823-39.